AIP | Applied Physics Letters

Room temperature sputtering of inclined c-axis ZnO for shear mode solidly mounted resonators

G. Rughoobur, M. DeMiguel-Ramos, T. Mirea, M. Clement, J. Olivares, B. Díaz-Durán, J. Sangrador, I. Miele, W. I. Milne, E. Iborra, and A. J. Flewitt

Citation: Applied Physics Letters **108**, 034103 (2016); doi: 10.1063/1.4940683
View online: http://dx.doi.org/10.1063/1.4940683
View Table of Contents: http://scitation.aip.org/content/aip/journal/apl/108/3?ver=pdfcov
Published by the AIP Publishing

Room temperature sputtering of inclined *c*-axis ZnO for shear mode solidly mounted resonators

G. Rughoobur,[1] M. DeMiguel-Ramos,[1] T. Mirea,[2] M. Clement,[2] J. Olivares,[2] B. Díaz-Durán,[2] J. Sangrador,[2] I. Miele,[1] W. I. Milne,[1,3] E. Iborra,[2] and A. J. Flewitt[1,a)]
[1]*Electrical Engineering Division, Department of Engineering, University of Cambridge, 9 JJ Thomson Avenue, Cambridge, CB3 0FA, United Kingdom*
[2]*GMME-CEMDATIC-ETSI de Telecomunicación, Universidad Politécnica de Madrid, 28040 Madrid, Spain*
[3]*College of Information Science and Electronic Engineering, Zhejiang University, Hangzhou, 310027, People's Republic of China*

(Received 21 December 2015; accepted 12 January 2016; published online 20 January 2016)

ZnO films with a *c*-axis significantly inclined away from the surface normal were grown by a remote plasma sputtering technique at room temperature. The films were used to make solidly mounted resonators (SMRs) operating in shear mode at a resonant frequency of 1.35 GHz. Control of the ZnO microstructure was achieved using a polycrystalline AlN seed layer which can be added on top of a sputtered acoustic mirror to give a complete SMR device. The ZnO was reactively sputtered in an atmosphere of argon and oxygen from a zinc target. The *c*-axis of the ZnO was estimated to be at an angle of ~45° to the surface normal. SMRs were measured to have quality factors (Q) of up to 140 and effective electromechanical coupling coefficients of up to 2.2% in air. Although an inclined *c*-axis can be achieved with direct growth onto the acoustic mirror, it is shown that the AlN seed layer provides higher coupling coefficients and narrower inclination angular distribution. The responses of the devices in liquids of different viscosities (acetone, water, and AZ5214E photoresist) were measured. The shear mode Q decreased by 45% in acetone, 72% in water, and 92% in AZ5214E. © *2016 AIP Publishing LLC*. [http://dx.doi.org/10.1063/1.4940683]

Recently, there has been a growing need for high sensitivity gravimetric sensors that can operate in liquid environments. In-liquid sensing can be achieved with the shear mode that has a significantly lower attenuation because the shear waves couple less into the liquid, and the energy losses are lower.[1] The quartz crystal microbalance (QCM) is a well-established technology where a shear mode is generated across the thickness of a quartz substrate.[2] However, the quartz substrates are thick (330–55 μm), consequently QCMs resonate at low frequencies (5–20 MHz).[2] This limits the maximum mass sensitivity of QCMs, which according to Sauerbrey is proportional to the square of the operating frequency.[3] For higher sensitivities, higher operating frequencies are necessary.[4] The quartz plates have to be made thinner, but this is expensive and the plates become very fragile. With thin film technology, piezoelectric materials such as ZnO and AlN have emerged as better alternatives to quartz as they can be reactively sputtered to the desired thickness for working at a determined high frequency in the 1–5 GHz range.[5,6] Thin piezoelectric films can also be used in contour mode resonators where the resonant frequency is dependent on the electrode geometry, but the low operating frequencies (~160 MHz) reduce mass sensitivities.[7] Thin film resonators are categorized by the structure used for acoustic energy confinement: the film bulk acoustic resonator (FBAR), made on a free membrane with air acting as the acoustic reflector and the solidly mounted resonator (SMR), which is fabricated on an acoustic reflector made of alternating high and low acoustic impedance material layers each with quarter wavelength thickness.[8]

Polycrystalline thin films of ZnO and AlN with good piezoelectricity–both of which crystallize in the wurtzite structure–are obtained when all the microcrystals have the same *c*-axis orientation and exhibit the same crystal polarity.[9] This is achieved during sputtering under certain conditions that favor the preferential growth of the (000·2) planes parallel to a given direction. In addition, the nature, roughness, and crystallographic orientation of the surface onto which the piezoelectric thin film is deposited are essential parameters for controlling the subsequent crystallographic and polar orientations of the piezoelectric film.[10] Usually, the *c*-axis of the grown film is normal to the substrate surface, and this results in the longitudinal acoustic mode operation. Whilst this mode can be used in FBARs and SMRs for gas sensing, it cannot be used in liquid environments due to efficient coupling of the energy of the longitudinal mode into the liquid. Confining the liquid within microfluidic channels reduces the dissipation partially in longitudinal modes.[11] However, the channel thickness needs to be designed as a multiple of half the acoustic wavelength for each liquid being sensed to reduce acoustic leakage. A shear mode is required instead for liquid environments. Lateral excitation of the shear mode through the d_{15} coefficient in *c*-axis oriented films consists of applying an electric field parallel to the surface of a *c*-axis textured film through two coplanar electrodes. In practice, the electric fields between the coplanar electrodes are weak, and excited shear modes have low electromechanical coupling coefficients (<0.01%) in SMRs.[12] Stronger shear resonances can be achieved by thickness excitation of films with the *c*-axis inclined with respect to the surface normal, through the component of the electric field perpendicular to the

a)Author to whom correspondence should be addressed. Electronic mail: ajf@eng.cam.ac.uk, Tel.: +44 1223 748332, Fax: +44 1223 748348.

c-axis and the d_{15} coefficient.[12] In order to effectively excite the shear mode, the polarization axis of the film should have an inclination angle between 20° and 50° from the surface normal.[13] Piezoelectric ZnO films with grains inclined away from the surface normal can be sputtered on substrates with controlled roughness so that the local surface on which the ZnO grains are nucleating is not parallel to the macroscopic plane of the substrates.[14,15] If the flux of atoms impinging on the exposed facets is constant, the grains of the piezoelectric material will grow in different directions, leading to a randomly oriented layer with poor piezoelectric characteristics. However, if the substrate is displaced away from the center of the target, an impinging direction is encouraged. Therefore, the grains will grow faster on the facets that are most exposed to the atom flux and their inclination angle will be more uniform.[16] A sawtooth surface profile is the best possible structure to achieve grains with a homogeneous inclination angle; yet such topography is difficult to fabricate. Instead, a layer with a textured surface is commonly used to grow piezoelectric films with inclined *c*-axis.

The focus of this work is to study the influence of two different surface textures in growing inclined *c*-axis ZnO at room temperature using a similar method for growing inclined AlN as reported previously by DeMiguel-Ramos *et al.*[16] Deposition is at room temperature which is attractive to ensure compatibility with device processing and for temperature sensitive substrates (polymers and flexible materials). AlN seed layers were deposited under specific conditions that promote the growth of (10·3) oriented grains; these show a faceted surface with adequate local surface that is not parallel to the macroscopic substrate surface. The possibility of utilizing the roughness generated after the acoustic reflector deposition as an alternative surface texture is also investigated. The shear mode performance has been measured by fabricating and characterizing SMRs.

First, five layers alternating between porous SiO_2[17] and Mo were deposited on a (1 0 0)-oriented Si substrate to form the acoustic mirror. The five reflector layers (three of SiO_2 and two of Mo) were sputtered in a pulsed DC Leybold Z550 system with 150 mm diameter targets of Si and Mo in Ar/O_2 mixtures and in pure Ar, respectively. The thicknesses (521 nm for SiO_2 and 629 nm for Mo) were designed so that the reflectors have a reflection band for the shear mode centered at 1.2 GHz. The surface roughness of one set of reflectors was reduced from around 20 nm to less than 1 nm by chemical mechanical polishing using alumina slurry. After sputtering 50 nm of Mo as the bottom electrode, the AlN seed (~100 nm) was deposited on the polished samples in an ultra-high vacuum sputtering system pumped down to a base pressure of 1.3×10^{-6} Pa to avoid oxygen contamination. A 150 mm diameter 99.999% purity Al target located at a distance of 55 mm from the substrate holder was used. The sputtering process was performed at a pressure of 0.67 Pa with a 60% N_2 in Ar admixture and a pulsed DC power of 600 W, without any intentional heating of the susbtrate; these conditions promote the growth of (10·3) oriented AlN microcrystals.[18,19] A high target utilisation sputtering (HiTUS) system was then used to reactively sputter the piezoelectric ZnO layer (800 nm thick) from a 100 mm diameter 99.999% Zn target in a 60% O_2 in Ar gas admixture, at a total pressure of 0.24 Pa.[20] A power of 1000 W from a 13.56 MHz RF supply generated the remote plasma and the Zn target was biased with a DC power of 800 W during the deposition. These conditions provided a sputtering rate of approximately 40 nm min^{-1} at the edge of the substrate holder. Off-axis deposition of the piezoelectric ZnO was achieved by reducing the distance separating the substrate holder and the target to 50 mm. Mo (~150 nm) was then deposited as the top electrode using a 99.95% target at a power of 100 W and pressure of 0.30 Pa in a DC magnetron sputtering system. Finally, this top electrode was defined using standard UV photolithography followed by a dry etch process with a CF_4/O_2 plasma.

X-ray diffraction (XRD) was used to determine the crystal orientation of the ZnO by measuring the polar patterns around the (000·2) reflection ($2\theta = 34.02°$). The resonators were characterized on a coplanar probe station with 150 μm pitch G-S-G RF probes (Picoprobes from GGB industries, USA) connected to an Agilent E5062A network analyzer in the frequency range from 0.5 to 3.0 GHz. The quality factors at resonant and anti-resonant frequencies ($Q_{r,a}$) and the effective coupling coefficient k^2_{eff} were calculated using

$$Q_{r,a} = \frac{f_{r,a}}{2}\frac{\mathrm{d}\phi_Y}{\mathrm{d}f}\bigg|_{f=f_{r,a}}, \tag{1}$$

$$k^2_{\text{eff}} = \frac{\pi f_r}{2 f_a}\frac{1}{\tan\left(\frac{\pi}{2}\frac{f_r}{f_a}\right)}, \tag{2}$$

where f_r is the resonant frequency, f_a is the anti-resonant frequency, and ϕ_Y is the phase of the electrical admittance, Y. The material electromechanical coupling coefficient, k^2_{mat}, of the ZnO for the shear resonance was extracted by fitting the experimental data with the Mason model.[21] In addition, liquids of different viscosities (acetone, de-ionised water, and AZ5214E photoresist) were added on top of the active area by means of a micro-pipette and the shear mode Q at resonance was extracted.

The exposed facets of the AlN seed layers were observed by scanning electron microscopy (SEM) (Figure 1(a)). The surface of an unpolished reflector (Figure 1(b)) demonstrated larger grains (~100 nm) compared to the AlN seed layers, which had grains of approximately 50 nm and a clear faceting. A cross-sectional cut of a device on the AlN seed layer is shown in Figure 1(c) and on a rough reflector is shown in Figure 1(d). These reveal an inclination of approximately 40° in the ZnO grains. The XRD polar measurements (Figure 2) confirm that the ZnO film on the AlN seed layer (Figure 2(a)) had a *c*-axis inclination of ~45° and a narrower tilt distribution compared to that deposited on the rough surface (Figure 2(b)), which had a mean inclination of only ~25° and a greater dispersion because of the more dispersed and less homogeneous local surface microscopic planes. Conversely, the substrates with AlN seed layers mainly had a (10·3) orientation showing uniformly distributed facets of the basal plane inclined ~31° from the normal to the substrate surface. These promote the growth of a more uniformly inclined layer.[16] ZnO films grown on surfaces with controlled roughness

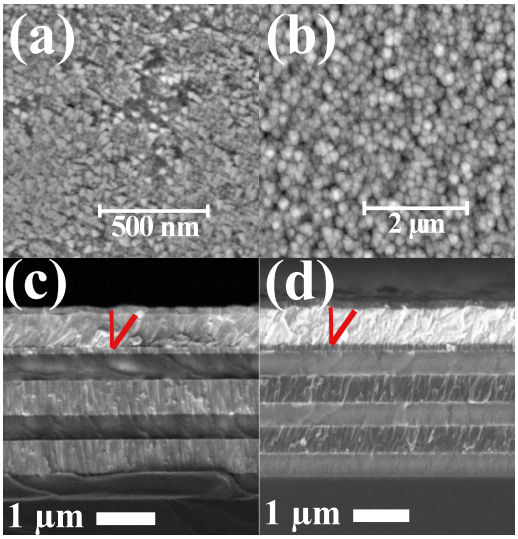

FIG. 1. SEM micrographs of surface and cross section of the devices. (a) The AlN seed layer with exposed (10·3) facets that promote the growth of the inclined ZnO; (b) the surface of the unpolished reflector with large grains (∼100 nm). (c) An inclined 800 nm ZnO sputtered on AlN and (d) an inclined 800 nm ZnO sputtered on rough surface. The Mo and SiO_2 layers from the reflector stack are also observed in (a) and (d).

therefore have high c-axis inclination angles without requiring significant and complex modifications to the deposition system outlined in other similar work.[15,22]

The electrical impedance spectra measured for a representative device from each set of resonators are shown in Figure 3. The devices exhibit appreciable shear and longitudinal modes but the frequencies were higher than the predicted value, because of thickness variation caused by the off-axis deposition. An estimate for the ratio of the longitudinal resonant frequency, f_r^L, to the shear mode resonant frequency, f_r^S, was calculated from the quasi-shear velocity, v^S, and quasi-longitudinal velocity, v^L, using

$$v^S = \left[\frac{c_{33}^* + c_{55}^*}{2\rho} - \left(\left(\frac{c_{33}^* - c_{55}^*}{2\rho}\right)^2 + \left(\frac{c_{35}^*}{\rho}\right)^2\right)^{0.5}\right]^{0.5}, \quad (3)$$

$$v^L = \left[\frac{c_{33}^* + c_{55}^*}{2\rho} + \left(\left(\frac{c_{33}^* - c_{55}^*}{2\rho}\right)^2 + \left(\frac{c_{35}^*}{\rho}\right)^2\right)^{0.5}\right]^{0.5}, \quad (4)$$

where c_{33}^*, c_{35}^*, and c_{55}^* are the piezoelectrically stiffened elastic constants of the rotated crystal and ρ is the density.[23] At an inclination angle of 25° for the rough reflector, the calculated ratio (v^L/v^S) of ZnO was 2.06, whereas at 45° for the AlN seed, this ratio was 1.95. These were close to the experimental frequency ratio of 2.10 ($f_r^S = 1.35$ GHz, $f_r^L = 2.67$ GHz) for the rough surface and 1.98 ($f_r^S = 1.36$ GHz, $f_r^L = 2.87$ GHz) for the AlN seed. Devices fabricated on rough substrates had longitudinal modes with k_{eff}^2 of only 0.95%. For comparison, values of k_{eff}^2 for the longitudinal mode of resonators fabricated with the same conditions on polished substrates located at the axis of the target (pure c-axis oriented films) are around 5.4% at 2.5 GHz. Therefore with the inclined grains the electrical energy couples less efficiently into the longitudinal mode

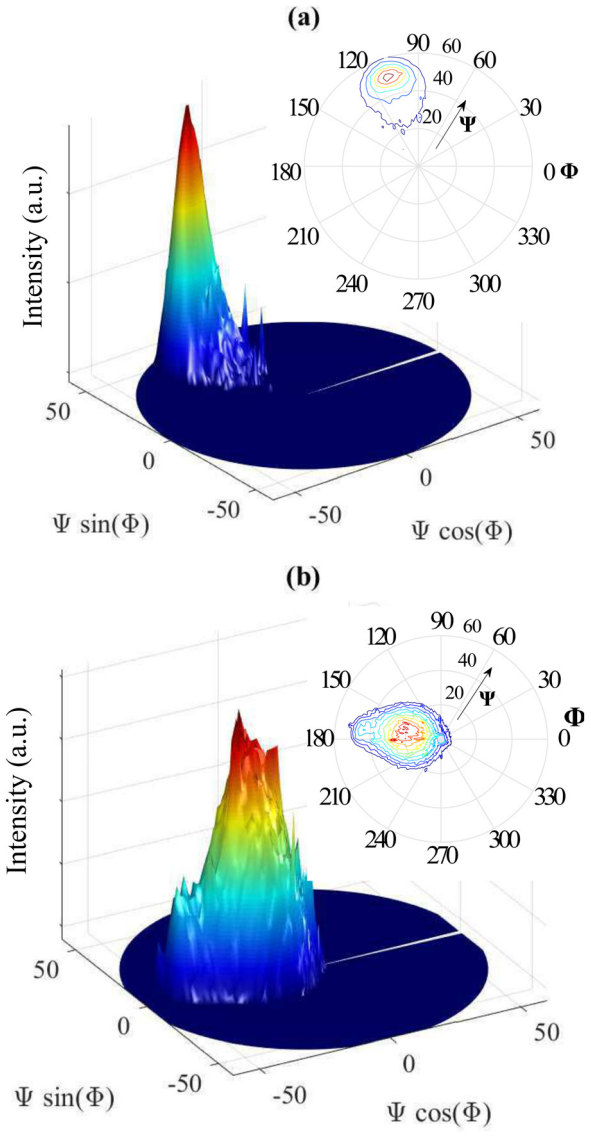

FIG. 2. Polar measurements of the angles in 3D representation and plan view for ZnO films deposited on (a) AlN seed with ∼45° inclination and narrower dispersion and (b) rough substrate with a 25° inclination and broader dispersion.

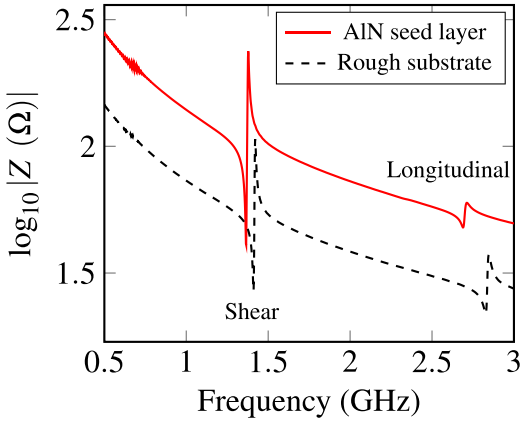

FIG. 3. Frequency response of the typical devices measured, the red line represents the device with AlN seed layer and the dashed black line shows the response of SMR with the rough reflector. Both set of devices demonstrate the shear and longitudinal modes, but devices on the rough reflector had a more pronounced longitudinal resonance.

TABLE I. Shear mode performance of typical devices measured.

Substrates	f_r^S (GHz)	Q_r	Q_a	k^2_{eff} (%)	k^2_{mat} (%)
AlN seed	1.350	139	116	2.22	2.09
Rough	1.364	115	102	1.35	1.31

and more into the shear resonance. The electromechanical performances outlined in Table I demonstrate that devices with ZnO grown on the AlN seed layers had higher k^2_{eff} (~2.2% at 1.35 GHz) compared to the rough substrates (~1.3% at 1.36 GHz). Growing ZnO on a layer of AlN with controlled orientation improves the homogeneity of the inclination angles in the ZnO, which explains the higher k^2_{eff} of the shear mode in those devices. However, the random roughness of the acoustic reflector surface leads to a greater range of inclination orientations as observed in the polar patterns (Figure 2(b)), which deteriorate the electromechanical performance of the resonator. The shear mode Q was low (80–140) compared with similar work with inclined c-axis ZnO without a seed layer.[22] A lower Q is equivalent to a broader resonance peak, which reduces the number of frequencies that can be resolved and hence limits the mass resolutions. However, the Q can be improved by using an electrode with a controlled roughness. This would eliminate the interfacial and scattering losses caused by either the random roughness of the acoustic mirror or the piezoelectrically "dead" AlN seed layer.

The effects of liquids with different products of viscosities (η) and densities (ρ) on the shear mode of a device with an AlN seed layer resonating at 1.35 GHz are shown in Figure 4. The shear mode Q decreases from 139 to 76 (by 45%) in acetone ($\rho = 0.79$ g cm^{-3}, $\eta = 0.3$ mPa s). In contrast, longitudinal mode Q (shown in Figure 5) is reduced by 87% in contact with acetone, thus rendering it unsuitable for in-liquid sensing. The shear mode Q decreased by 72% in water ($\rho = 1.00$ g cm^{-3}, $\eta = 1.0$ mPa s) and by 92% in AZ5214E ($\rho = 1.00$ g cm^{-3}, $\eta = 22$ mPa s). This Q decreased because

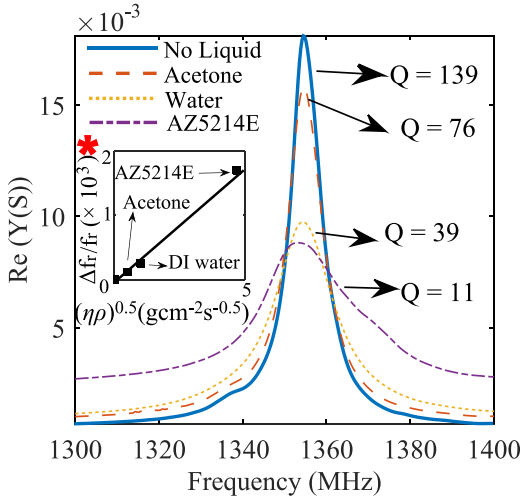

FIG. 4. Effect of liquids of different viscosities and densities on the shear resonance (of a device with AlN seed layer with shear mode at 1.35 GHz) demonstrating that when viscosity increases (acetone to AZ5214E photoresist), the Q decreases due to damping and the resonant frequency (inset denoted by *) decreases linearly with $(\eta\rho)^{0.5}$.

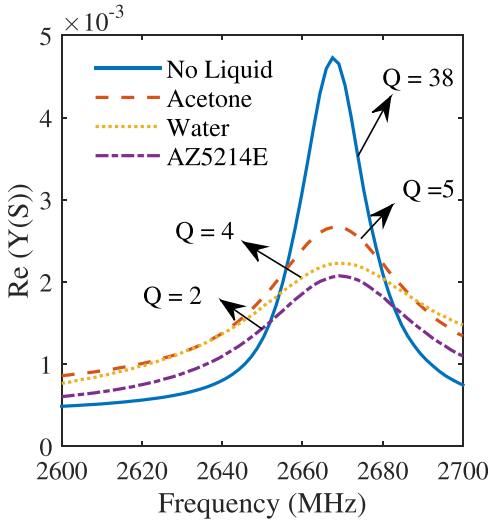

FIG. 5. Effect of liquids with different $(\eta\rho)^{0.5}$ on the longitudinal resonance (2.67 GHz) Q, which is decimated immediately by 87%, 90% and 95% in contact with acetone, water, and AZ5214E, respectively.

the shear modulus of the liquid is non-negligible when its viscosity increases and acoustic energy leaks into the liquid. A frequency shift is also observed in the shear resonance with liquids of different $\eta\rho$ products (see inset of Figure 4). This is caused by the mass loading of the liquid due to a greater adherence to the resonator surface as viscosity increases, which decreases the shear mode frequency.[24] The frequency shifts were proportional to $(\eta\rho)^{0.5}$ as predicted by the model of Kanazawa and Gordon for thickness shear mode in the QCMs.[25] Nonetheless the number of liquid measurements was limited to nine trials on average because of microcracking of the ZnO layer due to its porous nature and sensitivity to liquids, but this is acceptable for disposable sensors to which this technology is most suited. Having said that, capping with silicon oxide or silicon nitride outside the active area could solve this problem.

It has been shown that by using a surface with controlled roughness and an off-axis deposition, polycrystalline ZnO films with a controlled and uniform inclined c-axis were grown at room temperature, which is promising for process compatibility and plastic substrates.

The research leading to these results has received funding from the European Community's Horizon 2020 Programme under Grant Agreement No. SPIRE-01-2014-636820, the IC1208 Cost action, and from the Ministerio de Economía y Competitividad del Gobierno de España through the Project No. MAT2013-45957-R. Financial support from these institutions is therefore gratefully acknowledged. G.R. also wishes to acknowledge funding from the Cambridge Trust.

[1]G. Wingqvist, Surf. Coat. Technol. **205**(5), 1279 (2010).
[2]C. I. Cheng, Y.-P. Chang, and Y.-H. Chu, Chem. Soc. Rev. **41**(5), 1947–1971 (2012).
[3]G. Sauerbrey, Z. Phys. **155**(2), 206 (1959).
[4]S. W. Wenzel and R. M. White, Appl. Phys. Lett. **54**(20), 1976 (1989).
[5]H. Campanella, J. Esteve, J. Montserrat, A. Uranga, G. Abadal, N. Barniol, and A. Romano-Rodríguez, Appl. Phys. Lett. **89**(3), 033507 (2006).

[6]Z. Yan, X. Y. Zhou, G. K. H. Pang, T. Zhang, W. L. Liu, J. G. Cheng, Z. T. Song, S. L. Feng, L. H. Lai, J. Z. Chen, and Y. Wang, Appl. Phys. Lett. **90**(14), 143503 (2007).
[7]W. Xu, S. Choi, and J. Chae, Appl. Phys. Lett. **96**(5), 053703 (2010).
[8]R. Ruby, in *IEEE Ultrasonics Symposium, 2007* (2007), pp. 1029–1040.
[9]J. Ruffner, P. Clem, B. Tuttle, D. Dimos, and D. Gonzales, Thin Solid Films **354**, 256–261 (1999).
[10]Y. Lin, C. Hong, and H. Chuang, Appl. Surf. Sci. **254**(13), 3780–3786 (2008).
[11]W. Xu, X. Zhang, H. Yu, A. Abbaspour-Tamijani, and J. Chae, IEEE Electron Device Lett. **30**(6), 647–649 (2009).
[12]M. Clement, E. Iborra, J. Olivares, M. DeMiguel-Ramos, T. Mirea, and J. Sangrador, Ultrasonics **54**(6), 1504–1508 (2014).
[13]G. Wingqvist, J. Bjurström, A. Hellgren, and I. Katardjiev, Sens. Actuators, B **127**(1), 248 (2007).
[14]J. Weber, W. M. Albers, J. Tuppurainen, M. Link, R. Gabl, W. Wersing, and M. Schreiter, Sens. Actuators, A **128**(1), 84–88 (2006).
[15]T. Yanagitani, M. Kiuchi, M. Matsukawa, and Y. Watanabe, IEEE Trans. Ultrason., Ferroelectr., Freq. Control **54**(8), 1680–1686 (2007).
[16]M. DeMiguel-Ramos, T. Mirea, M. Clement, J. Olivares, J. Sangrador, and E. Iborra, Thin Solid Films **590**, 219–223 (2015).
[17]J. Olivares, E. Wegmann, J. Capilla, E. Iborra, M. Clement, L. Vergara, and R. Aigner, IEEE Trans. Ultrason., Ferroelect., Freq. Control **57**(1), 23–29 (2010).
[18]M. Clement, E. Iborra, J. Sangrador, A. Sanz-Hervaís, L. Vergara, and M. Aguilar, J. Appl. Phys. **94**(3), 1495 (2003).
[19]M. DeMiguel-Ramos, M. Clement, J. Olivares, J. Capilla, J. Sangrador, and E. Iborra, in *European Frequency and Time Forum International Frequency Control Symposium (EFTF/IFC), 2013 Joint* (IEEE, 2013).
[20]A. J. Flewitt, J. D. Dutson, P. Beecher, D. Paul, S. J. Wakeham, M. E. Vickers, C. Ducati, S. P. Speakman, W. I. Milne, and M. J. Thwaites, Semicond. Sci. Technol. **24**(8), 085002 (2009).
[21]J. F. Rosenbaum, *Bulk Acoustic Wave Theory and Devices* (Artech House, New York, 1945).
[22]M. Link, J. Weber, M. Schreiter, W. Wersing, O. Elmazria, and P. Alnot, Sens. Actuators, B **121**(2), 372–378 (2007).
[23]N. Foster, G. Coquin, G. Rozgonyi, and F. Vannatta, IEEE Trans. Sonics Ultrason. **15**(1), 28–40 (1968).
[24]L. Qin, Q. Chen, H. Cheng, Q. Chen, J.-F. Li, and Q.-M. Wang, J. Appl. Phys. **110**(9), 094511 (2011).
[25]K. K. Kanazawa and J. G. Gordon, Anal. Chem. **57**(8), 1770–1771 (1985).